

## M74 X-1 (CXOU J013651.1+154547): AN EXTREMELY VARIABLE ULTRALUMINOUS X-RAY SOURCE

M.I. KRAUSS<sup>1,3</sup>, R.E. KILGARD<sup>1,2</sup>, M.R. GARCIA<sup>1</sup>, T.P. ROBERTS<sup>2</sup>, AND A.H. PRESTWICH<sup>1</sup>*Draft version November 11, 2018*

## ABSTRACT

Ultraluminous X-ray sources (ULXs) have been described variously as the most luminous normal X-ray binaries, as hypernovae, and as “intermediate-mass” black holes with masses of hundreds to thousands of solar masses. We present results on M74 X-1 (CXOU J013651.1+154547), a ULX in the nearby spiral galaxy M74 (NGC 628), from observations by *Chandra* and *XMM-Newton*. M74 X-1 is a persistent source which exhibits extreme variability and changes in spectral state on timescales of several thousand seconds. Its variability timescales and behavior resemble some Galactic microquasars. This suggests that the emission mechanism may be related to relativistically beamed jets, and that M74 X-1 could be an extragalactic “microblazar”—a microquasar whose jet axis is aligned with our line of sight. We also note that its spectrum is consistent with the presence of a low-temperature disk blackbody component, which, assuming it is due to radiation from an accretion disk, could indicate that M74 X-1 contains an intermediate-mass black hole.

*Subject headings:* galaxies: individual (NGC 628, M74) — X-rays: individual (CXOU J013651.1+154547, M74 X-1)

## 1. INTRODUCTION

Ultraluminous X-ray sources (ULXs) are historically defined as point sources whose luminosities exceed the Eddington luminosity for a 10  $M_{\odot}$  compact object,  $L_x \simeq 10^{39}$  erg s<sup>-1</sup>. Although they were discovered in the *Einstein* era (Fabbiano 1989), and more than 100 ULX candidates were subsequently catalogued by the *ROSAT* HRI (Roberts & Warwick 2000; Colbert & Ptak 2002), much about the nature of these sources was unknown until recent times. Observatories such as *ASCA* provided valuable information about the spectra of ULXs (see, e.g., Makishima et al. 2000); however, except in the cases where the sources were significantly variable, there remained the possibility that what appeared to be a ULX was really a group of spatially unresolved sources.

The ability to spatially separate ULXs from their surrounding environs is now possible with the superb resolution of the *Chandra X-ray Observatory*, and both *Chandra* and *XMM-Newton* can perform high quality X-ray spectroscopy and temporal analysis. This affords us detailed insight into the nature of ULXs: we now know, for example, that probably 10% or fewer ULXs are associated with recent supernovae (Roberts et al. 2002), and that the others are, in fact, isolated sources. Although some ULXs are found in elliptical galaxies (Colbert & Ptak 2002), most reside in star forming and starburst galaxies, implying that they are associated with recent star formation (though the exact nature of this link is unclear).

A number of models have been proposed to explain the high X-ray luminosity of ULXs, and it is likely that more than one is required to explain all types of observed ULX activity. Some ULXs may be extragalactic microquasars (Körding, Falcke & Markoff 2002; Foschini et al. 2003; Georganopoulos, Aharonian & Kirk 2002; King et al. 2001), in which case the observed high

luminosities would be due to relativistic beaming. Others may be stellar-mass black holes with super-Eddington radiation (Begelman 2002). Some are almost certainly background AGN that happen to fall along the line-of-sight to the host galaxy (Irwin, Bregman, & Athey 2004). One of the most intriguing suggestions is that they are intermediate-mass black holes (IMBHs, see e.g. Colbert & Mushotzky 1999; Makishima et al. 2000; Miller et al. 2003). Aside from their high luminosities, the low-temperature blackbody component in some ULX spectra can be used to argue for the presence of an IMBH (Miller et al. 2003). In this scenario, the blackbody spectrum is assumed to arise from an accretion disk, and its temperature can be used to infer the radius of the disk’s inner edge and thus a mass for the central object.

In this paper we focus on observations of a specific ULX, M74 X-1 (CXOU J013651.1+154547). The first X-ray imaging observation of M74, which is at a distance of 8.7 Mpc (Huchra, Vogeley & Geller 1999), was obtained with the *Einstein* HRI on 1980 January 5. Though it is not included in the *Einstein* source catalog, there is a source present at the location of M74 X-1 with a 0.3–10 keV flux of  $7.6 \times 10^{-14}$  erg cm<sup>-2</sup> s<sup>-1</sup> (14 total counts), corresponding to a luminosity of  $7 \times 10^{38}$  erg s<sup>-1</sup>. M74 was also observed by *ASCA* on 1995 July 28, but no source is detected at the location of M74 X-1. We derive an upper limit to the 0.2–10 keV flux of  $7 \times 10^{-14}$  erg cm<sup>-2</sup> s<sup>-1</sup> (corresponding to a luminosity of  $6 \times 10^{38}$  erg cm<sup>-2</sup> s<sup>-1</sup>). No pointed *ROSAT* observations were performed.

The *Chandra* observations of M74 were conducted as part of a Cycle 2 large project to study the point source population of nearby, face-on spiral galaxies (Prestwich 2001). M74 X-1, one of the objects in a subsample of ultraluminous point sources, was discovered to be extremely variable and exhibit strong flares with a characteristic timescale of several thousand seconds. In Section 2, we report on the recent X-ray observations of M74 X-1; in particular, its spectral characteristics and variability. In Section 3 we present optical and radio ob-

<sup>1</sup> Harvard-Smithsonian Center for Astrophysics<sup>2</sup> University of Leicester<sup>3</sup> Massachusetts Institute of Technology

servations of M74. In Section 4, we discuss M74 X-1's location in M74, as well as its observed spectral and variability properties; and compare our findings with Galactic microquasars and with other ULXs.

## 2. X-RAY OBSERVATIONS AND DATA ANALYSIS

*Chandra* has observed M74 twice, on 2001 June 19 and 2001 October 19. Each observation utilized the ACIS back illuminated S3 chip, and basic processing was done by the *Chandra* X-ray Center (CXC). There are two small background flares in the first observation during which background rates jump to two and three times the quiescent level. These flares were not filtered out for analysis because they contribute a negligible ( $\sim 0.3$ ) number of counts to the source data presented here. The total duration of the “good time intervals” (GTIs) for the June dataset is 46.4 ks. There are no background flares in the October observation, whose GTIs sum to 46.2 ks. Both datasets have been filtered to include only energies in the range 0.3–10.0 keV.

*XMM-Newton* observed M74 for 36 ks on 2002 February 2. The data from MOS1, MOS2, and the PN were reduced individually, then fit simultaneously during spectral analysis, but were summed together for the temporal analysis. Data reduction was performed using SAS (Science Analysis Software) v5.3. Several significant background flares were removed for analysis, resulting in the loss of  $\sim 7$  ks of data. The data were also filtered for “good” events plus pattern  $\leq 12$  (MOS) and  $\leq 4$  (PN), and for the energy range 0.2–10.0 keV. The total duration of the GTIs are, for MOS1 and MOS2, 28.9 ks; and for the PN, 28.7 ks.

### 2.1. Spectral Fitting and Energetics

Spectral fits were performed using *Sherpa*, the fitting tool included in the CIAO data analysis package. Background data were subtracted prior to fitting. *powell* was used for optimization, and Chi Data Variance was the statistic function employed. The fits to the *Chandra* (*XMM*) data were performed on data grouped in 15 (20) count bins. The *Chandra* ARFs were corrected for the ACIS low energy QE degradation using the *corrarf* program.<sup>4</sup> In the *XMM* observation, M74 X-1 is 6' off-axis and close to chip gaps on all the detectors, so the tools *rmfgen* and *arfgen* were used to produce correct response files for fitting.

For the 2001 June 19 (*Chandra*) observation, there are a total of 347 source counts, of which approximately seven are due to background contamination. The 2001 October 19 (*Chandra*) observation contains a total of 963 source counts, of which approximately eight are due to background. Both source ellipses are of a size that is expected to contain 98% of the source energy, given their off-axis angle (3'6 for June, and 3'8 for October). For the 2002 February 2 (*XMM-Newton*) observation, a source-free background region on the same chip as the source was used for background determination. After background subtraction, there are a total of  $\sim 650$  counts in the PN spectrum and  $\sim 430$  counts in the MOS spectra.

At its peak brightness in the *Chandra* observations, the 0.3–10.0 keV count rate is 0.11 cts s<sup>-1</sup>, corresponding to

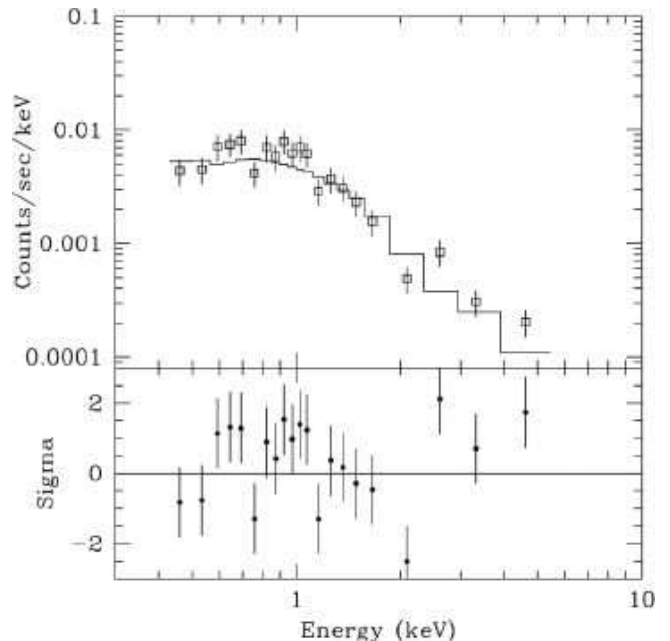


FIG. 1.— 2001 June 19 *Chandra* spectrum with the absorbed (Galactic  $N_H$ ) power-law fit overplotted and residuals shown below.

a source flux of  $1.3 \times 10^{-12}$  erg cm<sup>-2</sup> s<sup>-1</sup>, or a luminosity of  $1.2 \times 10^{40}$  erg s<sup>-1</sup>. To verify that the spectrum is not affected by pileup, we used the CIAO tool *mkpsf* to create a PSF image at the location of M74 X-1. The inner  $3 \times 3$  pixel region of the PSF contains 43.4% of the total flux, whereas this would be 88.6% were the source at the aimpoint of the detector. Using the pileup algorithm implemented in PIMMS (Portable, Interactive Multi-Mission Simulator), the source at its brightest (0.11 cts s<sup>-1</sup>) is 3.2% piled, while on average (a rate of 0.04 cts s<sup>-1</sup>) it is 1.2% piled. This will not cause a statistically significant change in the shape of the spectrum.

For initial spectral fitting, we tried a range of standard simple models, such as a disk blackbody, power-law, thermal bremsstrahlung, and MEKAL. Of these models, only the power-law provides acceptable fits (see Figures 1, 2, and 3). However, the 2001 October 19 spectrum still has significant residuals beyond the power-law fit. If we restrict the fitting range of the power-law to cover 1.5–10.0 keV, these residuals are manifested as a soft excess (see Figure 4). We were motivated by the spectra seen in Galactic X-ray binaries (and in other ULXs, c.f. Miller et al. 2003) to add a disk blackbody (DBB) component to the power-law, and using an *F*-test, we find that this improves the fit at the  $3.3\sigma$  level (see Figure 5). We find that the soft excess is similarly well-fit by a MEKAL model with low abundances and by a single-temperature blackbody spectrum. Using an *F*-test to compare these models with the power-law fit, we determine that the addition of a MEKAL component is favored at the  $3.7\sigma$  level, whereas the blackbody component is favored at the  $3.1\sigma$  level. We also fit the spectrum with a broken power-law model, but find that the parameters are not well constrained. We present the fit parameters for all the datasets in Tables 1 (power-law and power-law plus disk blackbody fits) and 2 (power-

<sup>4</sup> Information about *corrarf* can be found at [http://cxc.harvard.edu/cal/Links/Acis/acis/Cal\\_prods/qeDeg/](http://cxc.harvard.edu/cal/Links/Acis/acis/Cal_prods/qeDeg/).

TABLE 1  
POWER-LAW AND POWER-LAW PLUS DISK BLACKBODY SPECTRAL FITS<sup>a</sup>

Observation	$N_H$	Power-law			Disk Blackbody			$\chi^2_\nu$ (DOF, sig.)
	( $\times 10^{20}$ )	$\Gamma$	Amplitude <sup>b</sup> ( $\times 10^{-5}$ )	Flux <sup>c</sup> ( $\times 10^{-13}$ )	$kT_{in}$ (keV)	Norm	Flux <sup>c</sup> ( $\times 10^{-13}$ )	
2001 June 19	4.8	$2.25^{+0.19}_{-0.18}$	$0.96 \pm 0.09$	0.49	...	...	...	1.67 (19, N/A)
	$4^{+13}_{-4}$	$2.19^{+0.76}_{-0.38}$	$0.92^{+0.52}_{-0.20}$	0.48	...	...	...	1.75 (18, $0.2\sigma^{\S}$ )
	4.8	$0.6^{+0.9}_{-1.3}$	$0.17^{+0.31}_{-0.14}$	0.45	$0.29^{+0.07}_{-0.06}$	$0.22^{+0.31}_{-0.12}$	0.25	1.25 (17, $2.1\sigma^{\S}$ )
	$7^{+16}_{-7}$	$0.7^{+0.9}_{-1.6}$	$0.19^{+0.38}_{-0.17}$	0.45	$0.27^{+0.13}_{-0.10}$	$0.32^{+5.6}_{-0.26}$	0.27	1.32 (16, $2.0\sigma^{\dagger}$ )
	4.8	$2.02 \pm 0.10$	$2.72 \pm 0.15$	1.52	...	...	...	1.23 (55, N/A)
2001 Oct 19: All	$2.0^{+3.6}_{-2.0}$	$1.88^{+0.21}_{-0.17}$	$2.45^{+0.38}_{-0.28}$	1.49	...	...	...	1.22 (54, $1.1\sigma^{\S}$ )
	4.8	$1.1^{+0.4}_{-0.5}$	$1.0^{+0.6}_{-0.5}$	1.35	$0.27 \pm 0.05$	$0.6^{+0.6}_{-0.3}$	0.54	0.96 (53, $3.5\sigma^{\S}$ )
	$6^{+12}_{-6}$	$1.15^{+0.48}_{-0.71}$	$1.08^{+0.87}_{-0.70}$	1.36	$0.26^{+0.13}_{-0.10}$	$0.8^{+12.8}_{-0.6}$	0.56	0.98 (52, $3.3\sigma^{\dagger}$ )
	4.8	$1.77^{+0.17}_{-0.16}$	$5.18^{+0.47}_{-0.48}$	3.39	...	...	...	1.70 (27, N/A)
Bright:	$0^{+2.8}_{-N/A}$	$1.58^{+0.17}_{-0.14}$	$4.44^{+0.54}_{-0.40}$	3.44	...	...	...	1.58 (26, $1.7\sigma^{\S}$ )
	4.8	$0.67^{+0.50}_{-0.61}$	$1.6^{+1.4}_{-0.9}$	3.97	$0.29^{+0.08}_{-0.07}$	$1.0^{+1.8}_{-0.6}$	1.09	1.16 (25, $2.9\sigma^{\S}$ )
	$13^{+19}_{-13}$	$0.85^{+0.54}_{-0.88}$	$2.0^{+2.0}_{-1.5}$	3.93	$0.22^{+0.18}_{-0.08}$	$4.9^{+390}_{-4.7}$	1.7	1.19 (24, $2.5\sigma^{\dagger}$ )
	4.8	$0.83^{+0.55}_{-0.58}$	$1.8^{+1.6}_{-1.0}$	3.65	$0.31^{+0.05}_{-0.05}$	$0.69^{+0.58}_{-0.30}$	1.01	1.20 (25)
	4.8	$2.29^{+0.15}_{-0.14}$	$1.83^{+0.14}_{-0.14}$	0.93	...	...	...	0.86 (26, N/A)
Faint: <sup>d</sup>	$7.1^{+8.9}_{-7.1}$	$2.40^{+0.49}_{-0.40}$	$1.99^{+0.72}_{-0.51}$	0.99	...	...	...	0.88 (25, $0.6\sigma^{\S}$ )
	4.8	$0.83^{+0.55}_{-0.58}$	$0.29^{+0.37}_{-0.17}$	0.58	$0.31^{+0.05}_{-0.05}$	$0.33^{+0.34}_{-0.16}$	0.48	1.13 (26)
	4.8	$1.96^{+0.10}_{-0.09}$	$2.38 \pm 0.30$	1.4	...	...	...	1.09 (59, N/A)
2002 Feb 2	$1.1 \pm 2.7$	$1.77 \pm 0.17$	$2.09 \pm 0.34$	1.4	...	...	...	1.04 (58, $1.9\sigma^{\S}$ )
	4.8	$1.35 \pm 0.39$	$1.3 \pm 0.7$	1.3	$0.25 \pm 0.06$	$0.6 \pm 0.6$	0.3	0.92 (55, $2.6\sigma^{\S}$ )
	$1.2 \pm 6.3$	$1.24 \pm 0.52$	$1.1 \pm 0.8$	1.3	$0.31 \pm 0.16$	$0.2 \pm 0.4$	0.3	0.92 (54, $2.1\sigma^{\dagger}$ )

<sup>a</sup>Upper and lower limits are the 90% confidence range.  $N_H$  was frozen to the Galactic value of  $4.8 \times 10^{20} \text{ cm}^{-2}$  for fits where there is no  $N_H$  confidence range given; otherwise,  $N_H$  was allowed to vary without bound.

<sup>b</sup>The amplitudes of the power-laws are the flux at 1.0 keV in units of photons  $\text{keV}^{-1} \text{ cm}^{-2} \text{ s}^{-1}$ .

<sup>c</sup>0.3-10.0 keV flux in units of  $\text{erg cm}^{-2} \text{ s}^{-1}$ .

<sup>d</sup>Adding a disk blackbody component actually increased the value of  $\chi^2_\nu$  for these data.

<sup>†</sup>Significance is determined using an  $F$ -test comparing this fit to a power-law fit of the same data with  $N_H$  allowed to vary.

<sup>§</sup>Significance is determined using an  $F$ -test comparing this fit to a power-law fit of the same data with  $N_H$  frozen to the Galactic value.

<sup>†</sup>For these fits, the “faint” and “bright” data were fit using a common power-law slope and blackbody temperature, allowing only their normalizations to vary.

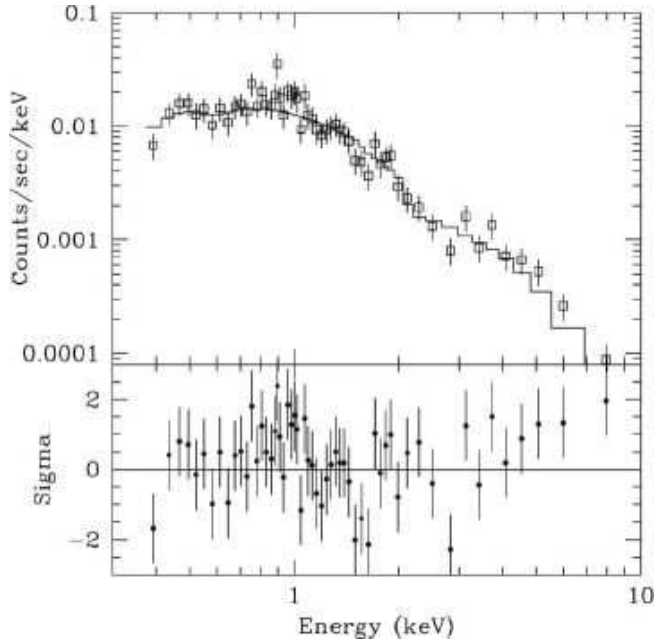


FIG. 2.— 2001 October 19 *Chandra* spectrum with the absorbed (Galactic  $N_H$ ) power-law fit overplotted and residuals shown below.

law plus MEKAL fits).

To explore possible spectral variability in the temporally variable October data (the lightcurve is presented in Figure 6), we separated it into “bright” (count rate  $> 0.03 \text{ cts s}^{-1}$ ) and “faint” (count rate  $< 0.03 \text{ cts s}^{-1}$ ) segments. Both segments had comparable numbers of counts; 490 in the bright data and 469 in the faint data, allowing for similar statistical properties. (There are an insufficient number of counts in the June observation to allow for a similar separation.) Fitting with simple power-laws, we find that the bright data are somewhat harder than the faint data: the best-fit photon index for the bright data is  $1.6^{+0.2}_{-0.1}$ , whereas for the faint data it is  $2.4^{+0.5}_{-0.4}$ . We also note that there appears to be a soft excess present in the bright data—as with the full dataset, this can be modeled variously with a disk blackbody, MEKAL component, and single-temperature blackbody. Although the spectra appear to be different, it is possible that the physical parameters of the system (for example, the power-law slope and blackbody temperature) remain the same as the source brightens, and that only the contributions of different components vary. To test this, we fit the bright and faint data simultaneously with an absorbed power-law plus a disk blackbody. We used a common power-law slope and disk blackbody tem-

TABLE 2  
POWER-LAW PLUS MEKAL SPECTRAL FITS<sup>a</sup>

Observation	$N_H$	Power-law			MEKAL				$\chi^2_\nu$ (DOF, sig.)
	( $\times 10^{20}$ )	$\Gamma$	Amplitude <sup>b</sup> ( $\times 10^{-5}$ )	Flux <sup>c</sup> ( $\times 10^{-13}$ )	Plasma Temp. (keV)	Abund.	Norm ( $\times 10^{-6}$ )	Flux <sup>c</sup> ( $\times 10^{-13}$ )	
2001 June 19	4.8	$1.93^{+0.33}_{-0.35}$	$0.76 \pm 0.18$	0.45	$0.25^{+1.1}_{-0.06}$	1	$3.0^{+2.3}_{-2.4}$	0.06	1.60 (17, $1.1\sigma^{\S}$ )
2001 Oct 19: All	4.8	$1.93^{+0.13}_{-0.14}$	$2.42^{+0.24}_{-0.25}$	1.43	$0.7^{+0.2}_{-0.4}$	1	$2.8^{+1.8}_{-1.7}$	0.08	1.15 (53, $1.9\sigma^{\S}$ )
	$0^{+2.1}_{-N/A}$	$1.68^{+0.15}_{-0.11}$	$1.95^{+0.26}_{-0.18}$	1.38	$0.7^{+0.2}_{-0.2}$	1	$3.3 \pm 1.5$	0.09	1.03 (52, $2.9\sigma^{\dagger}$ )
	4.8	$0.7^{+0.5}_{-0.6}$	$0.5^{+0.6}_{-0.3}$	1.30	$0.8 \pm 0.2$	$0.02^{+0.02}_{-0.01}$	$153^{+28}_{-32}$	0.72	0.90 (52, $3.6\sigma^{\S}$ )
	$2.8^{+5.1}_{-2.8}$	$0.7 \pm 0.6$	$0.6^{+0.7}_{-0.4}$	1.29	$0.8 \pm 0.2$	$0.02^{+0.04}_{-0.02}$	$126^{+95}_{-60}$	0.64	0.90 (51, $3.7\sigma^{\dagger}$ )
Bright:	4.8	$1.40^{+0.28}_{-0.29}$	$3.67^{+0.89}_{-0.87}$	3.44	$0.7 \pm 0.2$	1	$11.7 \pm 5.7$	0.32	1.40 (25, $2.1\sigma^{\S}$ )
	$0^{+2.4}_{-N/A}$	$1.30^{+0.23}_{-0.25}$	$3.31 \pm 0.69$	3.47	$0.7 \pm 0.2$	1	$9.9^{+4.9}_{-4.7}$	0.27	1.24 (24, $2.3\sigma^{\dagger}$ )
	4.8	$0.44^{+0.51}_{-0.63}$	$1.1^{+1.1}_{-0.7}$	4.02	$0.8 \pm 0.2$	$0.04^{+0.04}_{-0.03}$	$249^{+77}_{-85}$	1.29	0.98 (24, $3.3\sigma^{\S}$ )
	$0^{+8.1}_{-N/A}$	$0.56^{+0.48}_{-0.30}$	$1.3^{+1.1}_{-0.8}$	3.93	$0.8^{+0.3}_{-0.2}$	$0.06^{+0.06}_{-0.04}$	$160^{+200}_{-70}$	0.95	1.00 (23, $3.0\sigma^{\dagger}$ )

<sup>a</sup>Upper and lower limits are the 90% confidence range.  $N_H$  was frozen to the Galactic value of  $4.8 \times 10^{20} \text{ cm}^{-2}$  for fits where there is no  $N_H$  confidence range given; otherwise,  $N_H$  was allowed to vary without bound.

<sup>b</sup>The amplitudes of the power-laws are the flux at 1.0 keV in units of photons  $\text{keV}^{-1} \text{ cm}^{-2} \text{ s}^{-1}$ .

<sup>†</sup>Significance is determined using an  $F$ -test comparing this fit to a power-law fit of the same data with  $N_H$  allowed to vary.

<sup>§</sup>Significance is determined using an  $F$ -test comparing this fit to a power-law fit of the same data with  $N_H$  frozen to the Galactic value.

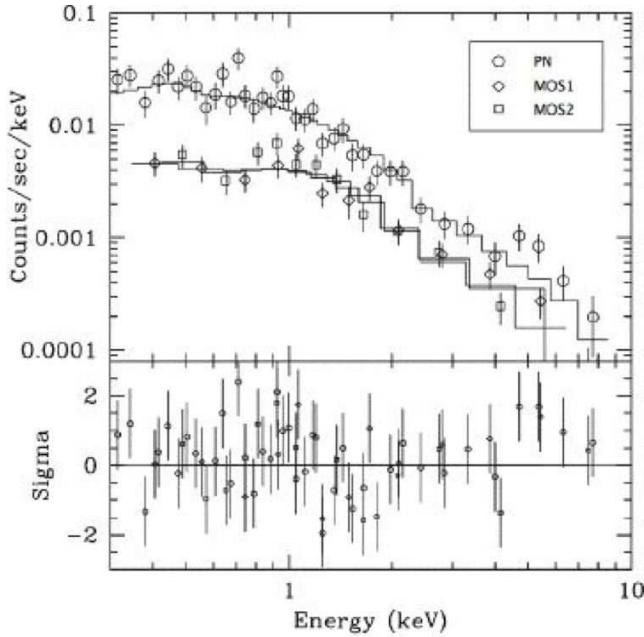


FIG. 3.— 2002 Feb 2 *XMM-Newton* spectrum with the power-law model (Galactic  $N_H$ ) overplotted and residuals shown below. PN data are plotted with circles, MOS1 data are plotted without a symbol, and MOS2 data are plotted with squares.

perature, and allowed only the normalizations to vary. Both datasets are consistent with a power-law slope of  $\Gamma = 0.8 \pm 0.6$  and a disk temperature of  $0.31^{+0.05}_{-0.05} \text{ keV}$ , but we must allow the amplitudes of both components to vary in order to get reasonable fits for the bright data. Plots of the “faint” and “bright” spectra are presented in Figures 7 and 8, and the results of spectral fitting are included in Tables 1 and 2.

To further explore the spectral variability, we plotted lightcurves of M74 X-1 in hard (1.0–10.0 keV) and soft (0.3–1.0 keV) bands. These lightcurves, along with a plot

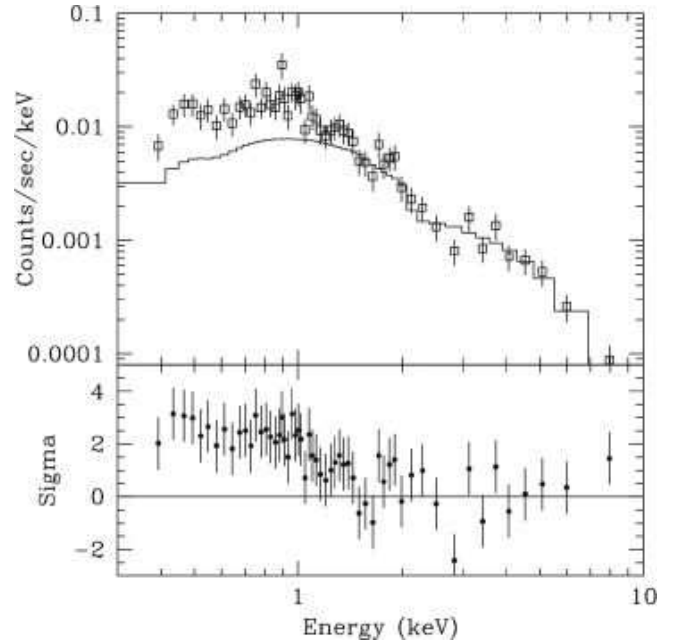


FIG. 4.— 2001 October 19 *Chandra* spectrum with a power-law fit over the restricted energy range 1.5–10 keV overplotted and residuals shown below.

of the hardness ratio, are presented in Figure 9. Unfortunately, the limited number of counts (and therefore the statistical noise) hinders detailed interpretation. Therefore, we also binned the data according to the source count rate, and calculated its hardness ratio. There appears to be a trend toward increasing hardness with higher count rate, as can be seen in Figure 10, although a linear fit with non-zero slope is preferred over a flat distribution at only the  $1.6\sigma$  level.

We performed a similar division of the 2002 February 2 dataset, but find that spectral hardening with increasing count rate is not present in these data.

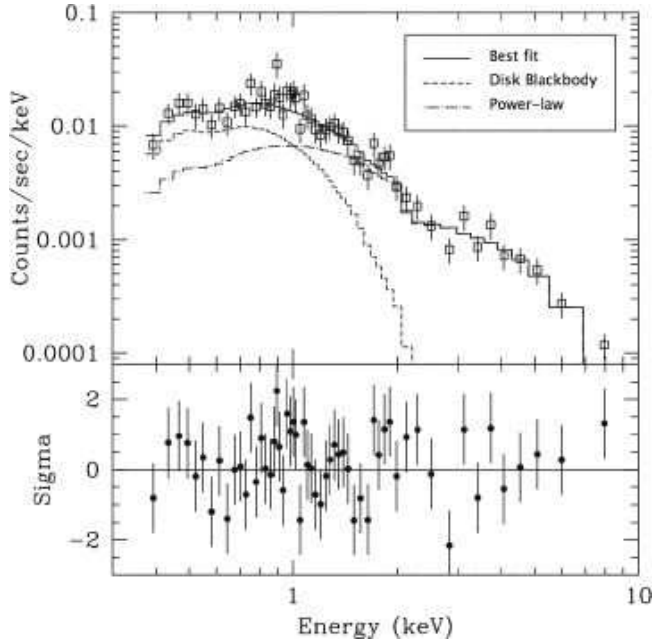


FIG. 5.— 2001 October 19 *Chandra* spectrum fit by a power-law plus disk blackbody. The fit and individual components are overplotted and residuals are shown below.

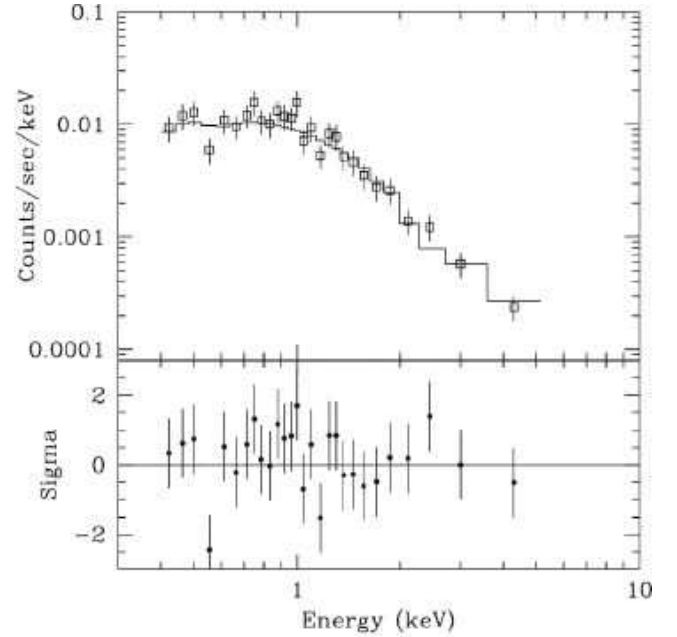


FIG. 7.— 2001 October 19 “faint” *Chandra* spectrum with the power-law model overplotted and residuals shown below.

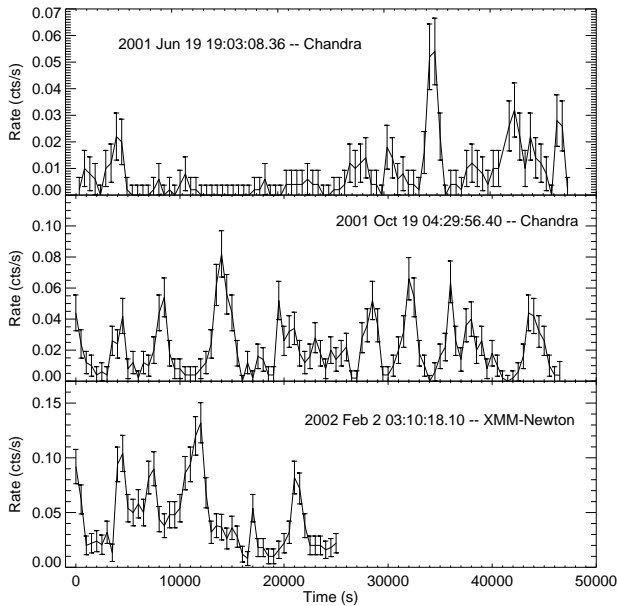


FIG. 6.— Lightcurves for all three observations. The data are binned by 500 s, and the full energy range (0.3–10.0 keV) has been used.

## 2.2. Variability

M74 X-1 is active and extremely variable in all three observations, with count rates sometimes increasing by an order of magnitude on a timescale of several thousand seconds. This variability is not caused or influenced by spacecraft dither or instrumental effects, and appears as a sequence of “flares”. The rise and decay of these flares generally appear symmetric, with a few exceptions when a flare is followed by a period of “noisy” decay (for example, after the fourth and seventh flares in the 2001

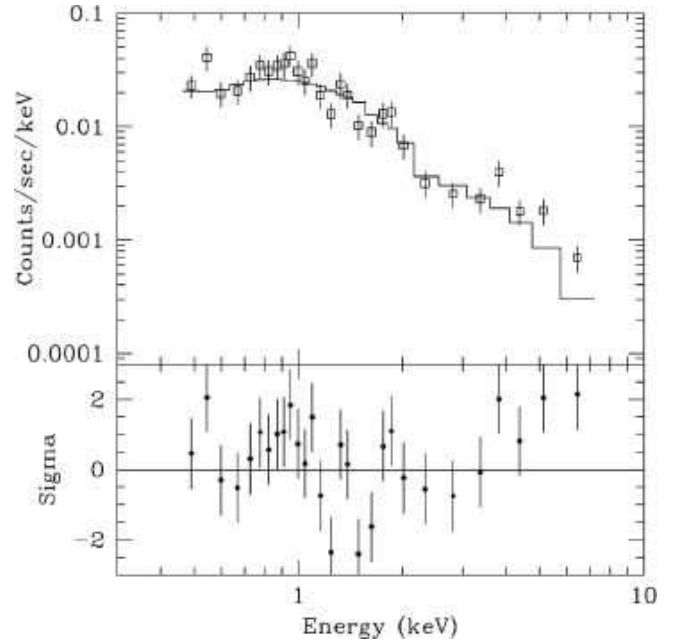


FIG. 8.— 2001 October 19 “bright” *Chandra* spectrum with the power-law model overplotted and residuals shown below.

October 19 data; see the lightcurves presented in Figure 6). The source is relatively inactive during the first half of the 2001 June 19 observation, but exhibits several significant flares in the latter half. It is active throughout the 2001 October 19 and 2002 February 2 observations; the former contains one particularly energetic flare during which the count rate rises from  $(0.004 \pm 0.003)$  cts  $s^{-1}$  to  $(0.08 \pm 0.01)$  cts  $s^{-1}$  in 2500 s.

An FFT reveals that there are a number of significant extremely low-frequency peaks (which could be interpreted as quasi-periodic oscillations, or QPOs) in the

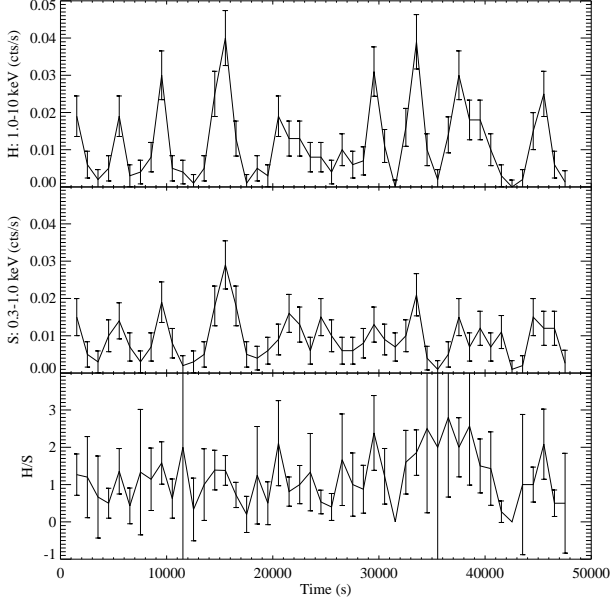


FIG. 9.— 2001 October 19 lightcurves in hard (1.0–10.0 keV) and soft (0.3–1.0 keV) bands, with the hardness ratio plotted below.

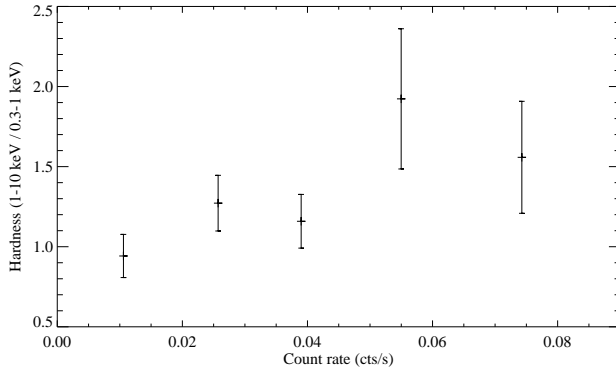


FIG. 10.— Hardness ratio (1.0–10.0 keV)/(0.3–1.0 keV) plotted against count rate for the 2001 October 19 data. Counts have been summed over specific count rate intervals in order to improve the statistics of the hardness ratios. A linear fit to the data shows that a line of slope 11 is preferred over a line of slope zero at the  $1.7\sigma$  level.

power spectrum of the October observation (see Figure 11). However, there are no significant peaks at higher frequencies up to the Nyquist frequency of 0.156 Hz in either of the *Chandra* observations, both of which have frame times of 3.2 s. Since the *XMM* PN data have time resolution of 73.4 ms (and a total of 660 counts), we searched it for higher frequency signals, but did not find anything significant. Performing period folding using the IRAF task `period` on all three of the observations produces  $\chi^2$  values for a range of periods (see Figure 12). There are broad peaks present in each, although there is not a single fundamental frequency.

### 3. OPTICAL AND RADIO DATA

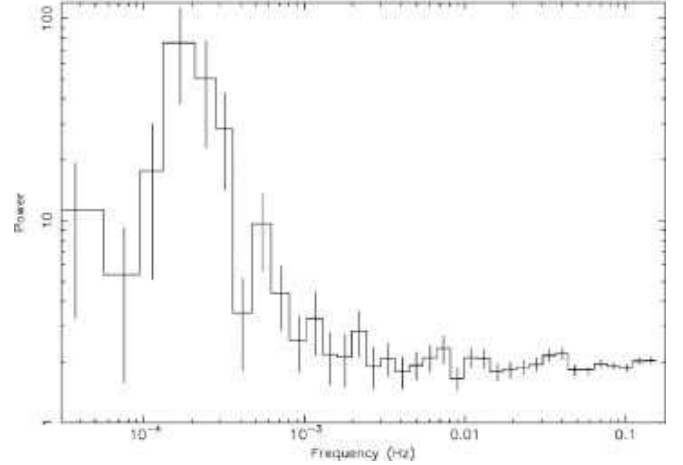


FIG. 11.— Normalized power density spectrum of the 2001 October 19 observation. The FFT was performed with a bin time of 3.241 s, and the frequency bins were averaged to improve the statistics.

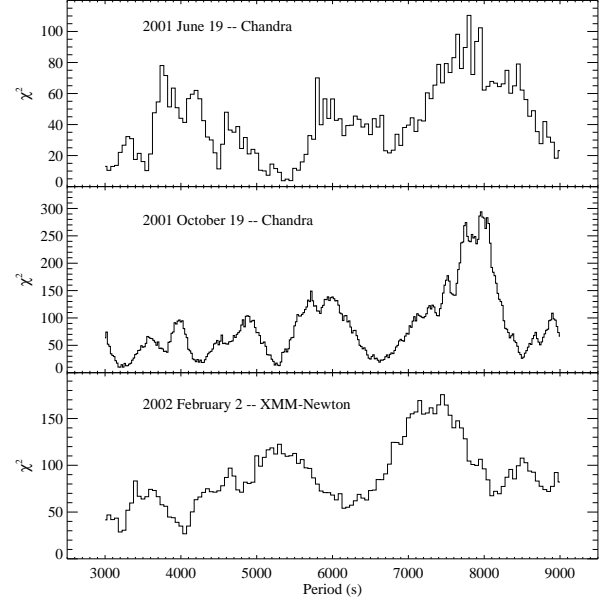


FIG. 12.— Period folding for all three observations. Folding was performed with the IRAF PROS routine `period` from 3000–9000 s with 50 s binning.

M74 was observed by the Gemini North telescope as part of its commissioning campaign with the GMOS detector on 2001 August 13–14. Four images in each filter—*G* (475 nm), *R* (630 nm), and *I* (780 nm)—were obtained and co-added for a total of 960, 480, and 480 s respectively. Basic processing was done at the Gemini Observatory. To register the world coordinate system (WCS) of the *R*-band image, we first extracted bright stars using the `SExtractor` program, then used the `imwcs` routine (both from the `WCSTools` package<sup>5</sup>) in conjunction with the USNO-A2.0 catalog to match 93 M74 sources to USNO-A2.0 objects. Sources in the *G*- and *I*-bands

<sup>5</sup> `WCSTools` documentation can be found at <http://tdc-www.harvard.edu/software/wcstools/>.

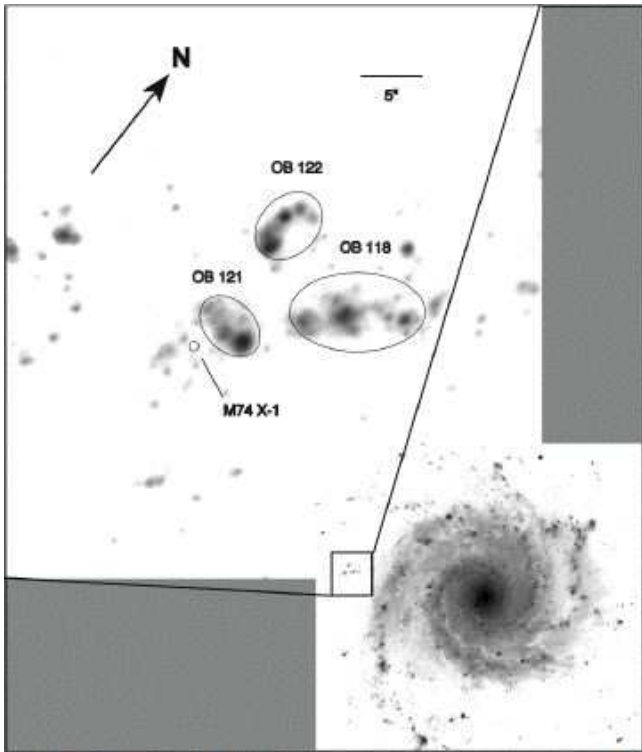


FIG. 13.— Gemini GMOS data (GRI image courtesy Gemini Observatory/GMOS team) overlaid with regions for OB associations 118, 121, and 122 (Ivanov et al. 1992) and the  $0.2''$  positional uncertainty of M74 X-1 (small circle).

were then centroided and these images were aligned to the  $R$ -band image using IRAF. After this process was complete, the centroids of three bright X-ray sources in the field which have optical counterparts fell within  $\pm 0''.2$  of them. Within the  $0''.2$  *Chandra* error circle there is no counterpart down to the limiting magnitude of  $m_V \simeq 25$  (calculated using the GMOS North Integration Time Calculator<sup>6</sup>, assuming a detection signal-to-noise threshold of 5.)

We also obtained observations of M74 taken on 2001 December 16 with the Fred Lawrence Whipple Observatory (FLWO) 1.2 m telescope. The galaxy was imaged in  $UBVRI$  (Harris broadband filter set), SII, and  $H\alpha$ . We note that there is no obvious ionization nebula present in either the SII or  $H\alpha$  images, as is sometimes observed in the vicinity of ULXs (Pakull & Mirioni 2002; Roberts et al. 2003). A Very Large Array (VLA) observation at 1.425 GHz did not reveal any radio counterpart with an upper limit of  $80 \mu\text{Jy}$  (Stockdale 2002). The X-ray flux density of the 2001 October 19 spectrum is  $4 \times 10^{-14} \text{ erg cm}^{-2} \text{ s}^{-1} \text{ keV}^{-1}$  at 1.0 keV, which gives a flux density of  $1.7 \times 10^{-2} \mu\text{Jy}$ . Given this X-ray flux, the lower limit to the X-ray-to-radio flux ratio is  $\log[F_X/F_R] > -3.8$ .

#### 4. DISCUSSION

M74 X-1 has some very unusual observational characteristics. It is a ULX (peak luminosity of  $1.2 \times$

$10^{40} \text{ erg s}^{-1}$ ) which is located near a young star cluster in M74. Its spectrum is reasonably fit by a simple power law, but in some observations there appears to be an excess at lower energies. This excess can be fit by a low temperature disk blackbody (0.3 keV) or a MEKAL model with low abundances. Its flux varies by an order of magnitude on timescales of half an hour, and there is tantalizing evidence for a QPO. The spectrum appears to harden as the source brightens, although the significance of this effect is low. In this section, we consider the physical interpretations for these observations.

##### 4.1. Location of M74 X-1

A major consideration in the study of ULXs is whether or not they actually reside in the galaxy with which they are coincident or whether they are, in fact, background or foreground sources. If M74 X-1 were in the Milky Way, given its Galactic latitude of  $-45.7$  and assuming it is 1.4 kpc above the Galactic plane (in the thick disk population), it would be at a distance of  $\sim 2$  kpc. If it were an LMXB, its counterpart would likely have  $4 \geq M_V \geq -4$  (van Paradijs & McClintock 1994), which at a distance of 2 kpc (and unobscured) would have  $15.5 \geq m_V \geq 7.5$ . Although the optical and X-ray observations were not simultaneous, the source seems to be X-ray active from June 2001 to February 2002, and two of the optical observations (Gemini and FLWO) were within this period. No object brighter than the  $m_V = 20.6$  OB association (or, in the Gemini data, any object at all within our error ellipse) is detected in any of the optical observations—we therefore consider it unlikely that M74 X-1 is a Galactic LMXB. Furthermore, it is unlikely that M74 X-1 is a Galactic cataclysmic variable, since large-amplitude X-ray oscillations of this type are most often seen in polars and intermediate polars, and would then be related to the spin period of the white dwarf. This would result in highly sinusoidal periodic variation. However, the observed variability is only quasi-periodic, and in June, the flares are only observed toward the end of the observation. Therefore, M74 X-1 most likely resides outside our Galaxy.

It is also possible that M74 X-1 is a background active galactic nucleus (AGN). Using equations 1 and 2 of Giaconini et al. (2001), and ignoring extinction from M74, it can be seen that zero to two sources of this flux would be expected on a single ACIS chip. If it were an AGN, it would most likely be a Narrow-Line Seyfert 1 (NLS1): these objects are highly X-ray variable, and are often not radio-loud—but note that they do have optical counterparts, unlike M74 X-1. Taking the detection limit of  $m_V = 25$  as the magnitude of the optical counterpart, the lower limit to the X-ray-to-optical flux ratio is  $\log[F_X/F_V] = 2.3$  (Maccacaro et al. 1982). Here, we assume no excess absorption—which would increase this ratio—since the absorption present in the spectra is always consistent with the Galactic value of  $N_H$ . Among AGN, BL Lac objects have the highest X-ray to optical flux ratio, ranging from  $\log[F_X/F_V] = 0.3$  to 1.7 (Stoeckle et al. 1991): this is significantly lower than what is observed for M74 X-1. Furthermore, there are only a few AGN which approach the variability exhibited by M74 X-1; for example, IRAS 13244–3809 (Dewangan et al. 2002; Boller et al. 1997) and PHL 1092 (Brandt et al. 1999). Since M74 X-1's extreme variability

<sup>6</sup> This calculator can be found at <http://www.gemini.edu/sciops/instruments/gmos/gmosIndex.html> following the Performance and Use link.



ity and lack of detected radio or optical counterpart all argue against its identification as a background AGN, we conclude that it almost certainly resides in M74.

#### 4.2. Limits on the binary system from optical data

Assuming that M74 X-1 is located in M74, the peak luminosity of  $1.2 \times 10^{40}$  erg s $^{-1}$  implies that M74 X-1 most likely contains a black hole, and probably has a binary companion. At the distance of M74, the detection limit of  $m_V \simeq 25$  corresponds to  $M_V \gtrsim -4.7$ ; thus any possible companion must be fainter than a B0III star ( $M_V \sim -4.9$ , de Jager & Nieuwenhuijzen 1987).

The Gemini data with the *Chandra* positional error circle and nearby OB associations overlaid are shown in Figure 13. M74 X-1 is near (but clearly not in) an OB association which has  $m_V = 20.6$  (OB 121, see Ivanov et al. 1992), consistent with a group of approximately 25 O or B stars. This is interesting, since ULXs are often located near star-forming regions (see, e.g. Zezas & Fabbiano 2002; Goad et al. 2002). Following a similar argument to that presented in Zezas & Fabbiano (2002), we consider the possibility that M74 X-1 is a binary which was ejected from the nearby star cluster OB 121. In this case, its projected separation of  $2''$  (corresponding to 85 pc) could be attained with a velocity in the plane of the sky of 30 km s $^{-1}$  for a period of approximately  $3 \times 10^6$  years. This velocity is not unexpected for stellar-mass black-hole binaries, given the observed velocities of such binaries and radio pulsars within our Galaxy. In fact, the velocity could be significantly higher; the Galactic microquasar GRO 1655–40 has a velocity of  $\sim 100$  km s $^{-1}$  (Mirabel et al. 2002)—adopting this value for M74 X-1 implies that it was ejected only  $\sim 8 \times 10^5$  years ago. The implied lifetime of  $\sim 10^6$  years is also compatible with the lifetime of the X-ray emitting phase of a  $M_{\text{BH}} \sim 10 M_\odot$  black-hole X-ray binary (Podsiadlowski, Rappaport & Han 2003). Taking the average luminosity of the system to be  $10^{39}$  erg s $^{-1}$ , the average  $\dot{M}$  is given by the equation  $\dot{M}_{\text{ave}} = L_{\text{ave}}/\eta c^2$ . Since  $\eta \sim 0.1$  for black hole systems,  $\dot{M} \sim 2 \times 10^{-7} M_\odot$  yr $^{-1}$ . Assuming that the primary is a black hole of  $10 M_\odot$ , this  $\dot{M}$  implies that  $M_2 \gtrsim 8 M_\odot$ , and the optical data imply that  $M_2 \lesssim 20 M_\odot$  (the lower limit is taken from Figure 4 of Podsiadlowski, Rappaport & Han 2003, and the upper limit is approximately the mass of an O9V or B0III star, both of which are at the luminosity limit for detection in the GMOS data). However, we caution that the peak luminosity of M74 X-1 is an order of magnitude higher than the Eddington limit for a  $10 M_\odot$  black hole; this is discussed further in the following sections. Finally, if M74 X-1 is a product of the recent star formation seen in the nearby OB associations, it is unlikely that it is in a system with a low-mass companion, since the secondary would not have had time to evolve off the main sequence and fill its Roche lobe. We conclude that M74 X-1 most likely has an intermediate- or high-mass donor if it is related to the nearby star-forming regions.

#### 4.3. Interpreting the soft excess

The spectra of M74 X-1 are reasonably fit, in most cases, by a power-law model, although in some cases the addition of a soft component (such as a blackbody) is favored with high ( $\gtrsim 3\sigma$ ) significance. Assuming that

this component is due to an accretion disk, we consider the physical implications of the fitted disk blackbody, which has an inner disk temperature of order 0.3 keV. The observed inner disk temperature in the 2001 October 19 “bright” data (0.29 keV) and disk blackbody luminosity ( $1.0 \times 10^{39}$  erg s $^{-1}$ ) imply an inner disk radius of  $\sim 1.2 \times 10^3$  km, which, if taken to be the innermost stable circular orbit of a non-spinning BH, requires a BH mass of  $\sim 140 M_\odot$  (Makishima et al. 2000, assuming a Schwarzschild BH.) Low-temperature disk blackbody components have also been seen in other ULXs, strengthening the hypothesis that they contain IMBHs (Miller et al. 2003).

Alternatively, if M74 X-1 is a stellar-mass black hole (which obeys the Eddington limit) then we might interpret its high luminosities as due to some sort of anisotropic emission process. As discussed in Section 4.1, the location of the M74 X-1 near OB 121 is consistent with an ejected black hole X-ray binary with a primary mass of  $10 M_\odot$ . In this case, the  $T_{\text{in}}$  of  $\sim 0.3$  keV can be compared to the  $\sim 1$  keV value found in Galactic BHXN when they are accreting at their Eddington rate (Makishima et al. 2000). If the disk extends down to the last stable orbit, this lower temperature implies a lower mass accretion rate,  $T_{\text{in}} \sim \dot{M}^{1/4}$  (Frank, King & Raine 1992, equation 5.41), which implies that  $\dot{M}$  is approximately 100 times below Eddington. Given that the observed peak disk blackbody luminosity is approximately the Eddington luminosity, this implies that M74 X-1 is beamed by a factor of  $b \sim 0.01$ , where  $b = \Omega/4\pi$ . This is more than one would expect from simple scattering of the flux off the inner edge of a funnel shaped accretion disk (King et al. 2001).

It is therefore difficult to reconcile the high luminosity of M74 X-1 and the low temperature of the thermal component without concluding that M74 X-1 is an intermediate-mass black hole. However, the presence of a thermal component is not necessarily due to an accretion disk. Some portion of the soft flux may be due to another process, such as X-rays scattered in an optically-thick outflow (Mukai et al. 2003). Or, it may be due to hot diffuse gas associated with the source. This interpretation is supported by the fact that the soft component is also fit well by a MEKAL model (see, e.g., Roberts et al. 2004 for a discussion of the physical interpretation of MEKAL components in ULX spectra).

#### 4.4. Spectral and temporal variability and the jet model

There is some evidence that the 2001 October 19 spectrum of M74 X-1 hardens as it becomes brighter (see the discussion in Section 2.1). Note that similar behavior has been observed in other ULXs: for example, a number of ULXs in NGC 4038/9 (the Antennae) harden with increasing flux (Fabbiano et al. 2003), as does NGC 6946 X-11 (MF 16; Roberts & Colbert 2003). Fabbiano et al. (2003) posit that this is due to an increase in the temperature of the inner disk at very high accretion rates. However, this model is not consistent with our observations of M74 X-1, since its spectrum is consistently dominated by the power-law component and since the variability occurs on extremely short timescales. Roberts & Colbert (2003) suggest two possible models for the hardening seen in NGC 6946 X-11—



that it may be due to variable emission from the base of a jet (Georganopoulos, Aharonian & Kirk 2002), or that it may be due to magnetic reconnection events in the accretion disk corona (di Matteo 1998). We favor the jet model for M74 X-1, since it also allows for the possibility of relativistic boosting of the X-rays and thus an amplification of the intrinsic variability. Relativistic beaming is a widely accepted explanation for many of the properties of face-on AGN, and several Galactic jet sources have also demonstrated variability that may be consistent with beamed X-ray emission: XTE J1650–500 (Tomsick et al. 2003) and SAX J1819.3–2525 (V4641 Sgr, Wijnands & van der Klis 2000).

M74 X-1 exhibits flares which appear relatively equally spaced, and an FFT of the October observation shows that there is a significant broad peak in the low-frequency range of the power spectrum. However, there is no coherent period, as can also be seen by the multiple peaks in Figure 12. We therefore rule out periodic sources for the variability, such as an orbital or spin modulation. We consider the possibility of eclipses of the inner disk by clumpy material to be unlikely, since there is no indication of an increase in  $N_{\text{H}}$  during the low-count-rate periods (it is consistent with the Galactic value throughout). It is also unlikely that the variability is due to jet precession, since it should then be strictly periodic, which it is not; furthermore, the timescales are very short compared with, for example, the 164 day precession period seen in SS 433 (Margon 1984). However, aperiodic variability of this kind could be related to processes at the base of the jet, namely the ejection of relativistic plasma into the jet. While such processes are not well understood, there is an observed correlation between activity in the inner disk and at the base of the jet in the Galactic microquasar GRS 1915+105, which happens on timescales similar to what is observed in M74 X-1 (see Section 4.5 for further discussion).

In each of its three observations, M74 X-1 is extremely variable and exhibits powerful X-ray flares—its luminosity fluctuates by an order of magnitude on timescales of half an hour. This is suggestive of beaming due to a relativistic jet: as seen in BL Lac objects (commonly called blazars), relativistic beaming along the line of sight leads to rapid, high-amplitude variability. M74 X-1 may, in fact, be a “microblazar”—a microquasar whose relativistic jet is beaming the X-ray emission towards us along the line of sight.

#### 4.5. Comparison with other ULXs and Galactic microquasars

Of Galactic sources, M74 X-1 closely resembles microquasars in both its temporal variability and energetics. A link between microquasars and ULXs has been posited by a number of authors (Körding, Falcke & Markoff 2002; Georganopoulos, Aharonian & Kirk 2002, for example); and recently, radio emission was discovered from a ULX in NGC 5408 (Kaaret et al. 2003). This radio emission is almost certainly due to a relativistic jet, and given the high radio flux, it is likely beamed, with a Doppler factor  $\delta = \gamma^{-1}(1 - \beta \cos \theta)^{-1} \gtrsim 5.8$ . The authors point out that this is consistent with the known ejecta velocities of GRS 1915+105, which would produce such a Doppler factor given a jet axis tilted up to  $10^\circ$  with respect to the line of sight (they further note that approximately 1 in 70

extragalactic microquasars should be thus aligned). The X-ray spectrum of the NGC 5408 source is also consistent with beamed emission, as it is well fit with a broken power-law model (but is also reasonably fit by a disk blackbody of 0.1 keV plus a power-law).

GRS 1915+105 is very similar to M74 X-1 in its temporal characteristics as well as its persistence. It has been active since its discovery in 1992, exhibiting a wide range of behavior (see, e.g., Muno, Morgan & Remillard 1999; Markwardt, Swank & Taam 1999). In some observations, GRS 1915+105 has been observed to vary from  $5 \times 10^{38}$  to  $3.5 \times 10^{39}$  erg s $^{-1}$  (Markwardt, Swank & Taam 1999, assuming  $D = 12.5$  kpc). This can be compared to M74 X-1, which has been active since 1980, and varies from  $\sim 5 \times 10^{38}$  to  $1.2 \times 10^{40}$  erg s $^{-1}$ . Although the low disk temperature and higher peak luminosities observed in M74 X-1 favor a larger black hole mass, the flares seen in M74 X-1 occur on the same timescales as some flaring behavior seen in GRS 1915+105, suggesting a similar dynamical timescale and thus similar physical scale.

Although much of the 0.3–10.0 keV X-ray emission from GRS 1915+105 is thought to come from its disk, there is also evidence for a correlation between disk emission and jet formation (Mirabel et al. 1998; Eikenberry et al. 1998). Therefore, the timescale for the variability at the base of the jet is likely similar to what is seen in X-ray observations. The jets of GRS 1915+105 are not directed toward our line of sight, but are inclined by  $70^\circ$  (Mirabel & Rodríguez 1994). If a jet were directed toward us, we would expect to see relativistically boosted emission varying on similar timescales to what is currently observed: we propose this scenario as a possible explanation for the high-amplitude flares seen in M74 X-1.

Another prominent feature of Galactic microquasars is their activity at radio wavelengths, which includes variability on timescales of tens of minutes to several hours. The radio flux of GRS 1915+105 has been observed to be as high as 430 mJy at 3.6 cm (Rodríguez & Mirabel 1997), but at the distance of M74 this would only be 0.8  $\mu$ Jy—unfortunately, not detectable by any current radio telescopes. Even if M74 X-1 were as radio-bright as the source in NGC 5408, at the distance of M74, it would be at the limit of detectability. As mentioned above, a search for radio emission in a 1.425 GHz VLA observation did not find emission at the location of M74 X-1 with an upper limit of 80  $\mu$ Jy.

## 5. SUMMARY AND CONCLUSIONS

M74 X-1 is a highly variable X-ray source whose 0.3–10.0 keV luminosity is seen to vary from approximately  $5 \times 10^{38}$  to  $1.2 \times 10^{40}$  erg s $^{-1}$  in several thousand seconds. It was detected by *Einstein* in 1980, and observed twice with *Chandra* and once with *XMM-Newton*. The latter three observations of M74 X-1 were each separated by approximately four months. There have also been a number of optical observations and a radio observation of the region, but as of yet, no counterpart has been found. Since M74 X-1 has no optical counterpart and is extremely variable, it is most likely in M74 (and thus a ULX), and may be related to the nearby OB association. In addition, its proximity to an OB association (a relatively common occurrence for ULXs) implies that it is likely a high- or intermediate-mass system.

The spectrum of M74 X-1 is consistent with a low temperature ( $\sim 0.3$  keV) disk blackbody component which has been observed in other ULXs. This component is often interpreted as arising from an accretion disk; its low temperature then implies an inner disk radius of  $1.2 \times 10^3$  km and therefore a black hole primary of mass  $140 M_{\odot}$ . However, in many ways M74 X-1 resembles stellar-mass Galactic microquasars. In this scenario, the very high X-ray luminosity and high-amplitude rapid variability would be produced by beaming from a jet which is aligned close to our line of sight. If M74 X-1 is, in fact, a stellar-mass black hole of mass  $\sim 10 M_{\odot}$ , it becomes difficult to explain the low temperature component in terms of an accretion disk, and it may be from a different physical source.

M74 X-1 is an intriguing object. It appears to be a black hole intermediate- or high-mass X-ray binary where the mass of the black hole remains an open question. We favor an interpretation in which M74 X-1 harbors a stellar mass black hole and the high observed X-ray luminosity is produced by beaming. However, we cannot

rule out an intermediate-mass black hole interpretation with the current data.

## 6. ACKNOWLEDGMENTS

We would like to thank the anonymous referees for many helpful comments and suggestions. We thank Jeff McClintock, Phil Kaaret, Andreas Zezas, Andrew King, Joe Patterson, Saul Rappaport, Albert Kong, Peter Freeman, Sebastian Heinz, Sera Markoff, Edo Berger and Chris Stockdale for helpful comments and discussion. MRG thanks the Aspen Center for Physics for its hospitality. We also thank the CXC SDS and DS teams, the *XMM-Newton* team, and the Gemini Observatory/GMOS team. Part of this work was based on observations obtained with *XMM-Newton*, an ESA science mission with instruments and contributions directly funded by ESA Member States and the USA (NASA). This work was partially supported by NASA contract NAS 8-39073 (CXC) and grant GO1-2092A.

## REFERENCES

- Begelman, M. 2002 ApJ, 568, L97  
 Boller, Th., Brandt, W. N., Fabian, A. C., & Fink, H. H. 1997, MNRAS, 289, 393  
 Brandt, W. N., Boller, Th., Fabian, A. C., & Ruszkowski, M. 1999, MNRAS, 303, L53  
 Colbert, E. J. M., & Mushotzky, R. F. 1999, ApJ, 519, 89  
 Colbert, E. J. M., & Ptak, A. F. 2002, ApJS, 143, 25  
 de Jager, C. & Nieuwenhuijzen, H. 1987, A&A, 177, 217  
 Dewangan, G. C., Boller, Th., Singh, K. P., & Leighly, K. M. 2002, A&A, 390, 65  
 di Matteo, T. 1998, MNRAS, 299, L15  
 Eikenberry, S. S., Matthews, K., Morgan, E. H., Remillard, R. A., & Nelson, R. W. 1998, ApJ, 494, L61  
 Esin, A., McClintock, J., & Narayan, R. 1997, ApJ, 489, 865  
 Fabbiano, G. 1989, ARA&A, 27, 87  
 Fabbiano, G., Zezas, A., King, A. R., Ponman, T. J., Rots, A. & Schweizer, F. 2003, ApJ, 584, L5  
 Foschini, L., Malaguti, G., Di Cocco, G., Cappi, M., Dadina, M. & Ho, L. C. 2003, in the Proceedings of the 15th SIGRAV Conference on General Relativity and Gravitation (astro-ph/0302143)  
 Frank, J., King, A., & Raine, D. 1992 Accretion Power in Astrophysics, (2d ed., Cambridge: Cambridge Univ. Press)  
 Georganopoulos, M., Aharonian, F. A. & Kirk, J. G. 2002 A&A, 388, L25  
 Giacconi, R. et al. 2001, ApJ, 551, 624  
 Goad, M. R., Roberts, T. P., Knigge, C., & Lira, P. 2002, MNRAS, 335, L67  
 Huchra, J. P., Vogeley, M. S., & Geller, M. J. 1999, ApJS, 121, 287  
 Irwin, J. A., Bregman, J. N., & Athey, A. E. 2004, ApJ, 601, L143  
 Ivanov, G. R., Popravko, G., Efremov, Yu. N., Tichonov, N. A., & Karachentsev, I. D. 1992, Astronomy & Astrophysics Supplement Series, 96, 645  
 Kaaret, P., Corbel, S., Prestwich, A. H. & Zezas, A. 2003, Science, 299, 365  
 King, A. R., Davies, M. B., Ward, M. J., Fabbiano, G., & Elvis, M. 2001a, ApJ, 552, L109  
 K rding, E., Falcke, H. & Markoff, S. 2002 A&A, 382, L13  
 Maccacaro et al. 1982, ApJ, 253, 504  
 Madau, P. & Rees, M. J. 2001, ApJ, 551, L27  
 Makishima, K. et al. 2000, ApJ, 535, 632  
 Margon, B. 1984, ARA&A, 22, 507  
 Markwardt, C. B., Swank, J. H., & Taam, R. E. 1999, ApJ, 513, L37  
 Miller, J. M., Fabbiano, G., Miller, M. C. & Fabian, A. C. 2003 ApJ, 585, L37  
 Mirabel, I. F. & Rodr guez, L. F. 1994 Nat., 371, 46  
 Mirabel, I. F., Dhawan, V., Chaty, S., Rodr guez, L. F., Marti, J., Robinson, C. R., Swank, J., Geballe, T. 1998, A&A, 330, L9  
 Mirabel, I. F., Mignani, R., Rodrigues, I., Combi, J. A., Rodr guez, L. F. & Guglielmetti, F. 2002, A&A, 395, 595  
 Morgan, E. H., Remillard, R. A., & Greiner, J. 1997, ApJ, 482, 993  
 Mukai, K., Pence, W. D., Snowden, S. L. & Kuntz, K. D. 2003, ApJ, 582, 184  
 Munro, M. P., Morgan, E. H., & Remillard, R. A. 1999, ApJ, 527, 321  
 Pakull, M. & Mirioni, L. 2002, in Jansen, F. et al., eds, New Visions of the X-ray Universe in the *XMM-Newton* and *Chandra* Era (astro-ph/0202488)  
 Podsiadlowski, Ph., Rappaport, S. & Han, Z. 2003, MNRAS, 341, 385  
 Prestwich, A. 2001, in Schlegel, E. M. & Vrtilik, S., eds, High Energy Universe at Sharp Focus: *Chandra* Science (ASP Conference Series)  
 Roberts, T. P., & Warwick, R. S. 2000, MNRAS, 315, 98  
 Roberts, T. P., Goad, M. R., Ward, M. J., Warwick, R. S., & Lira, P. 2002a, in Jansen, F. et al., eds, New Visions of the X-ray Universe in the *XMM-Newton* and *Chandra* Era (astro-ph/0202017)  
 Roberts, T. P., Goad, M. R., Ward, M. J. & Warwick, R. S. 2003, MNRAS, 342, 709  
 Roberts, T. P. & Colbert, E. J. M. 2003, MNRAS, 341, L49  
 Roberts, T. P., Warwick, R. S., Ward, M. J., & Goad, M. R. 2004, MNRAS, 349, 1193  
 Rodr guez, L. F. & Mirabel, I. F. 1997, ApJ, 474, L123  
 Stockdale, C. 2002, private communication  
 Stocke, J. T., Morris, S. L., Gioia, I. M., Maccacaro, T., Schild, R., Wolter, A., Fleming, T. A., & Henry, J. P. 1991, ApJS, 76, 813  
 Tomsick, J. A., Kalemci, E., Corbel, S. & Kaaret, P. 2003, ApJ, 592, 1100  
 van Paradijs, J. & McClintock, J. E. 1994, A&A, 290, 133  
 Wijnands, R. & van der Klis, M. 2000, ApJ, 528, L93  
 Zezas, A. & Fabbiano, G. 2002, ApJ, 577, 726